Search for CP violation in the decay τ^{-}→π^{-}K_{s}^{0}(≥Oπ^{0})ν_{τ}

J. P. Lees *et al.* (BABAR Collaboration)

Phys. Rev. D **85**, 031102 — Published 13 February 2012

DOI: 10.1103/PhysRevD.85.031102

BABAR-PUB-11/009
SLAC-PUB-14556

Search for *CP* Violation in the Decay $\tau^- \to \pi^- K^0_S\,(\geq 0\pi^0)\,\nu_\tau$

J. P. Lees,[1] V. Poireau,[1] V. Tisserand,[1] J. Garra Tico,[2] E. Grauges,[2] M. Martinelli[ab],[3] D. A. Milanes[a],[3] A. Palano[ab],[3] M. Pappagallo[ab],[3] G. Eigen,[4] B. Stugu,[4] D. N. Brown,[5] L. T. Kerth,[5] Yu. G. Kolomensky,[5] G. Lynch,[5] H. Koch,[6] T. Schroeder,[6] D. J. Asgeirsson,[7] C. Hearty,[7] T. S. Mattison,[7] J. A. McKenna,[7] A. Khan,[8] V. E. Blinov,[9] A. R. Buzykaev,[9] V. P. Druzhinin,[9] V. B. Golubev,[9] E. A. Kravchenko,[9] A. P. Onuchin,[9] S. I. Serednyakov,[9] Yu. I. Skovpen,[9] E. P. Solodov,[9] K. Yu. Todyshev,[9] A. N. Yushkov,[9] M. Bondioli,[10] D. Kirkby,[10] A. J. Lankford,[10] M. Mandelkern,[10] D. P. Stoker,[10] H. Atmacan,[11] J. W. Gary,[11] F. Liu,[11] O. Long,[11] G. M. Vitug,[11] C. Campagnari,[12] T. M. Hong,[12] D. Kovalskyi,[12] J. D. Richman,[12] C. A. West,[12] A. M. Eisner,[13] J. Kroseberg,[13] W. S. Lockman,[13] A. J. Martinez,[13] T. Schalk,[13] B. A. Schumm,[13] A. Seiden,[13] C. H. Cheng,[14] D. A. Doll,[14] B. Echenard,[14] K. T. Flood,[14] D. G. Hitlin,[14] P. Ongmongkolkul,[14] F. C. Porter,[14] A. Y. Rakitin,[14] R. Andreassen,[15] M. S. Dubrovin,[15] Z. Huard,[15] B. T. Meadows,[15] M. D. Sokoloff,[15] L. Sun,[15] P. C. Bloom,[16] W. T. Ford,[16] A. Gaz,[16] M. Nagel,[16] U. Nauenberg,[16] J. G. Smith,[16] S. R. Wagner,[16] R. Ayad,[17,*] W. H. Toki,[17] B. Spaan,[18] M. J. Kobel,[19] K. R. Schubert,[19] R. Schwierz,[19] D. Bernard,[20] M. Verderi,[20] P. J. Clark,[21] S. Playfer,[21] D. Bettoni[a],[22] C. Bozzi[a],[22] R. Calabrese[ab],[22] G. Cibinetto[ab],[22] E. Fioravanti[ab],[22] I. Garzia[ab],[22] E. Luppi[ab],[22] M. Munerato[ab],[22] M. Negrini[ab],[22] L. Piemontese[a],[22] V. Santoro,[22] R. Baldini-Ferroli,[23] A. Calcaterra,[23] R. de Sangro,[23] G. Finocchiaro,[23] M. Nicolaci,[23] P. Patteri,[23] I. M. Peruzzi,[23,†] M. Piccolo,[23] M. Rama,[23] A. Zallo,[23] R. Contri[ab],[24] E. Guido[ab],[24] M. Lo Vetere[ab],[24] M. R. Monge[ab],[24] S. Passaggio[a],[24] C. Patrignani[ab],[24] E. Robutti[a],[24] B. Bhuyan,[25] V. Prasad,[25] C. L. Lee,[26] M. Morii,[26] A. J. Edwards,[27] A. Adametz,[28] J. Marks,[28] U. Uwer,[28] F. U. Bernlochner,[29] M. Ebert,[29] H. M. Lacker,[29] T. Lueck,[29] P. D. Dauncey,[30] M. Tibbetts,[30] P. K. Behera,[31] U. Mallik,[31] C. Chen,[32] J. Cochran,[32] W. T. Meyer,[32] S. Prell,[32] E. I. Rosenberg,[32] A. E. Rubin,[32] A. V. Gritsan,[33] Z. J. Guo,[33] N. Arnaud,[34] M. Davier,[34] G. Grosdidier,[34] F. Le Diberder,[34] A. M. Lutz,[34] B. Malaescu,[34] P. Roudeau,[34] M. H. Schune,[34] A. Stocchi,[34] G. Wormser,[34] D. J. Lange,[35] D. M. Wright,[35] I. Bingham,[36] C. A. Chavez,[36] J. P. Coleman,[36] J. R. Fry,[36] E. Gabathuler,[36] D. E. Hutchcroft,[36] D. J. Payne,[36] C. Touramanis,[36] A. J. Bevan,[37] F. Di Lodovico,[37] R. Sacco,[37] M. Sigamani,[37] G. Cowan,[38] D. N. Brown,[39] C. L. Davis,[39] A. G. Denig,[40] M. Fritsch,[40] W. Gradl,[40] A. Hafner,[40] E. Prencipe,[40] K. E. Alwyn,[41] D. Bailey,[41] R. J. Barlow,[41,‡] G. Jackson,[41] G. D. Lafferty,[41] E. Behn,[42] R. Cenci,[42] B. Hamilton,[42] A. Jawahery,[42] D. A. Roberts,[42] G. Simi,[42] C. Dallapiccola,[43] R. Cowan,[44] D. Dujmic,[44] G. Sciolla,[44] D. Lindemann,[45] P. M. Patel,[45] S. H. Robertson,[45] M. Schram,[45] P. Biassoni[ab],[46] A. Lazzaro[ab],[46] V. Lombardo[a],[46] N. Neri[ab],[46] F. Palombo[ab],[46] S. Stracka[ab],[46] L. Cremaldi,[47] R. Godang,[47,§] R. Kroeger,[47] P. Sonnek,[47] D. J. Summers,[47] X. Nguyen,[48] P. Taras,[48] G. De Nardo[ab],[49] D. Monorchio[ab],[49] G. Onorato[ab],[49] C. Sciacca[ab],[49] G. Raven,[50] H. L. Snoek,[50] C. P. Jessop,[51] K. J. Knoepfel,[51] J. M. LoSecco,[51] W. F. Wang,[51] K. Honscheid,[52] R. Kass,[52] J. Brau,[53] R. Frey,[53] N. B. Sinev,[53] D. Strom,[53] E. Torrence,[53] E. Feltresi[ab],[54] N. Gagliardi[ab],[54] M. Margoni[ab],[54] M. Morandin[a],[54] M. Posocco[a],[54] M. Rotondo[a],[54] F. Simonetto[ab],[54] R. Stroili[ab],[54] S. Akar,[55] E. Ben-Haim,[55] M. Bomben,[55] G. R. Bonneaud,[55] H. Briand,[55] G. Calderini,[55] J. Chauveau,[55] O. Hamon,[55] Ph. Leruste,[55] G. Marchiori,[55] J. Ocariz,[55] S. Sitt,[55] M. Biasini[ab],[56] E. Manoni[ab],[56] S. Pacetti[ab],[56] A. Rossi[ab],[56] C. Angelini[ab],[57] G. Batignani[ab],[57] S. Bettarini[ab],[57] M. Carpinelli[ab],[57,¶] G. Casarosa[ab],[57] A. Cervelli[ab],[57] F. Forti[ab],[57] M. A. Giorgi[ab],[57] A. Lusiani[ac],[57] B. Oberhof[ab],[57] E. Paoloni[ab],[57] A. Perez[a],[57] G. Rizzo[ab],[57] J. J. Walsh[a],[57] D. Lopes Pegna,[58] C. Lu,[58] J. Olsen,[58] A. J. S. Smith,[58] A. V. Telnov,[58] F. Anulli[a],[59] G. Cavoto[a],[59] R. Faccini[ab],[59] F. Ferrarotto[a],[59] F. Ferroni[ab],[59] M. Gaspero[ab],[59] L. Li Gioi[a],[59] M. A. Mazzoni[a],[59] G. Piredda[a],[59] C. Bünger,[60] O. Grünberg,[60] T. Hartmann,[60] T. Leddig,[60] H. Schröder,[60] R. Waldi,[60] T. Adye,[61] E. O. Olaiya,[61] F. F. Wilson,[61] S. Emery,[62] G. Hamel de Monchenault,[62] G. Vasseur,[62] Ch. Yèche,[62] D. Aston,[63] D. J. Bard,[63] R. Bartoldus,[63] C. Cartaro,[63] M. R. Convery,[63] J. Dorfan,[63] G. P. Dubois-Felsmann,[63] W. Dunwoodie,[63] R. C. Field,[63] M. Franco Sevilla,[63] B. G. Fulsom,[63] A. M. Gabareen,[63] M. T. Graham,[63] P. Grenier,[63] C. Hast,[63] W. R. Innes,[63] M. H. Kelsey,[63] H. Kim,[63] P. Kim,[63] M. L. Kocian,[63] D. W. G. S. Leith,[63] P. Lewis,[63] S. Li,[63] B. Lindquist,[63] S. Luitz,[63] V. Luth,[63] H. L. Lynch,[63] D. B. MacFarlane,[63] D. R. Muller,[63] H. Neal,[63] S. Nelson,[63] I. Ofte,[63]

M. Perl,[63] T. Pulliam,[63] B. N. Ratcliff,[63] A. Roodman,[63] A. A. Salnikov,[63] R. H. Schindler,[63] A. Snyder,[63] D. Su,[63] M. K. Sullivan,[63] J. Va'vra,[63] A. P. Wagner,[63] M. Weaver,[63] W. J. Wisniewski,[63] M. Wittgen,[63] D. H. Wright,[63] H. W. Wulsin,[63] A. K. Yarritu,[63] C. C. Young,[63] V. Ziegler,[63] W. Park,[64] M. V. Purohit,[64] R. M. White,[64] J. R. Wilson,[64] A. Randle-Conde,[65] S. J. Sekula,[65] M. Bellis,[66] J. F. Benitez,[66] P. R. Burchat,[66] T. S. Miyashita,[66] M. S. Alam,[67] J. A. Ernst,[67] R. Gorodeisky,[68] N. Guttman,[68] D. R. Peimer,[68] A. Soffer,[68] P. Lund,[69] S. M. Spanier,[69] R. Eckmann,[70] J. L. Ritchie,[70] A. M. Ruland,[70] C. J. Schilling,[70] R. F. Schwitters,[70] B. C. Wray,[70] J. M. Izen,[71] X. C. Lou,[71] F. Bianchi[ab],[72] D. Gamba[ab],[72] L. Lanceri[ab],[73] L. Vitale[ab],[73] F. Martinez-Vidal,[74] A. Oyanguren,[74] H. Ahmed,[75] J. Albert,[75] Sw. Banerjee,[75] H. H. F. Choi,[75] G. J. King,[75] R. Kowalewski,[75] M. J. Lewczuk,[75] I. M. Nugent,[75] J. M. Roney,[75] R. J. Sobie,[75] N. Tasneem,[75] T. J. Gershon,[76] P. F. Harrison,[76] T. E. Latham,[76] E. M. T. Puccio,[76] H. R. Band,[77] S. Dasu,[77] Y. Pan,[77] R. Prepost,[77] and S. L. Wu[77]

(The *BABAR* Collaboration)

[1]*Laboratoire d'Annecy-le-Vieux de Physique des Particules (LAPP), Université de Savoie, CNRS/IN2P3, F-74941 Annecy-Le-Vieux, France*
[2]*Universitat de Barcelona, Facultat de Fisica, Departament ECM, E-08028 Barcelona, Spain*
[3]*INFN Sezione di Bari[a]; Dipartimento di Fisica, Università di Bari[b], I-70126 Bari, Italy*
[4]*University of Bergen, Institute of Physics, N-5007 Bergen, Norway*
[5]*Lawrence Berkeley National Laboratory and University of California, Berkeley, California 94720, USA*
[6]*Ruhr Universität Bochum, Institut für Experimentalphysik 1, D-44780 Bochum, Germany*
[7]*University of British Columbia, Vancouver, British Columbia, Canada V6T 1Z1*
[8]*Brunel University, Uxbridge, Middlesex UB8 3PH, United Kingdom*
[9]*Budker Institute of Nuclear Physics, Novosibirsk 630090, Russia*
[10]*University of California at Irvine, Irvine, California 92697, USA*
[11]*University of California at Riverside, Riverside, California 92521, USA*
[12]*University of California at Santa Barbara, Santa Barbara, California 93106, USA*
[13]*University of California at Santa Cruz, Institute for Particle Physics, Santa Cruz, California 95064, USA*
[14]*California Institute of Technology, Pasadena, California 91125, USA*
[15]*University of Cincinnati, Cincinnati, Ohio 45221, USA*
[16]*University of Colorado, Boulder, Colorado 80309, USA*
[17]*Colorado State University, Fort Collins, Colorado 80523, USA*
[18]*Technische Universität Dortmund, Fakultät Physik, D-44221 Dortmund, Germany*
[19]*Technische Universität Dresden, Institut für Kern- und Teilchenphysik, D-01062 Dresden, Germany*
[20]*Laboratoire Leprince-Ringuet, Ecole Polytechnique, CNRS/IN2P3, F-91128 Palaiseau, France*
[21]*University of Edinburgh, Edinburgh EH9 3JZ, United Kingdom*
[22]*INFN Sezione di Ferrara[a]; Dipartimento di Fisica, Università di Ferrara[b], I-44100 Ferrara, Italy*
[23]*INFN Laboratori Nazionali di Frascati, I-00044 Frascati, Italy*
[24]*INFN Sezione di Genova[a]; Dipartimento di Fisica, Università di Genova[b], I-16146 Genova, Italy*
[25]*Indian Institute of Technology Guwahati, Guwahati, Assam, 781 039, India*
[26]*Harvard University, Cambridge, Massachusetts 02138, USA*
[27]*Harvey Mudd College, Claremont, California 91711*
[28]*Universität Heidelberg, Physikalisches Institut, Philosophenweg 12, D-69120 Heidelberg, Germany*
[29]*Humboldt-Universität zu Berlin, Institut für Physik, Newtonstr. 15, D-12489 Berlin, Germany*
[30]*Imperial College London, London, SW7 2AZ, United Kingdom*
[31]*University of Iowa, Iowa City, Iowa 52242, USA*
[32]*Iowa State University, Ames, Iowa 50011-3160, USA*
[33]*Johns Hopkins University, Baltimore, Maryland 21218, USA*
[34]*Laboratoire de l'Accélérateur Linéaire, IN2P3/CNRS et Université Paris-Sud 11, Centre Scientifique d'Orsay, B. P. 34, F-91898 Orsay Cedex, France*
[35]*Lawrence Livermore National Laboratory, Livermore, California 94550, USA*
[36]*University of Liverpool, Liverpool L69 7ZE, United Kingdom*
[37]*Queen Mary, University of London, London, E1 4NS, United Kingdom*
[38]*University of London, Royal Holloway and Bedford New College, Egham, Surrey TW20 0EX, United Kingdom*
[39]*University of Louisville, Louisville, Kentucky 40292, USA*
[40]*Johannes Gutenberg-Universität Mainz, Institut für Kernphysik, D-55099 Mainz, Germany*
[41]*University of Manchester, Manchester M13 9PL, United Kingdom*
[42]*University of Maryland, College Park, Maryland 20742, USA*
[43]*University of Massachusetts, Amherst, Massachusetts 01003, USA*
[44]*Massachusetts Institute of Technology, Laboratory for Nuclear Science, Cambridge, Massachusetts 02139, USA*
[45]*McGill University, Montréal, Québec, Canada H3A 2T8*
[46]*INFN Sezione di Milano[a]; Dipartimento di Fisica, Università di Milano[b], I-20133 Milano, Italy*
[47]*University of Mississippi, University, Mississippi 38677, USA*
[48]*Université de Montréal, Physique des Particules, Montréal, Québec, Canada H3C 3J7*

[49]INFN Sezione di Napoli[a]; Dipartimento di Scienze Fisiche,
Università di Napoli Federico II[b], I-80126 Napoli, Italy
[50]NIKHEF, National Institute for Nuclear Physics and High Energy Physics, NL-1009 DB Amsterdam, The Netherlands
[51]University of Notre Dame, Notre Dame, Indiana 46556, USA
[52]Ohio State University, Columbus, Ohio 43210, USA
[53]University of Oregon, Eugene, Oregon 97403, USA
[54]INFN Sezione di Padova[a]; Dipartimento di Fisica, Università di Padova[b], I-35131 Padova, Italy
[55]Laboratoire de Physique Nucléaire et de Hautes Energies,
IN2P3/CNRS, Université Pierre et Marie Curie-Paris6,
Université Denis Diderot-Paris7, F-75252 Paris, France
[56]INFN Sezione di Perugia[a]; Dipartimento di Fisica, Università di Perugia[b], I-06100 Perugia, Italy
[57]INFN Sezione di Pisa[a]; Dipartimento di Fisica,
Università di Pisa[b]; Scuola Normale Superiore di Pisa[c], I-56127 Pisa, Italy
[58]Princeton University, Princeton, New Jersey 08544, USA
[59]INFN Sezione di Roma[a]; Dipartimento di Fisica,
Università di Roma La Sapienza[b], I-00185 Roma, Italy
[60]Universität Rostock, D-18051 Rostock, Germany
[61]Rutherford Appleton Laboratory, Chilton, Didcot, Oxon, OX11 0QX, United Kingdom
[62]CEA, Irfu, SPP, Centre de Saclay, F-91191 Gif-sur-Yvette, France
[63]SLAC National Accelerator Laboratory, Stanford, California 94309 USA
[64]University of South Carolina, Columbia, South Carolina 29208, USA
[65]Southern Methodist University, Dallas, Texas 75275, USA
[66]Stanford University, Stanford, California 94305-4060, USA
[67]State University of New York, Albany, New York 12222, USA
[68]Tel Aviv University, School of Physics and Astronomy, Tel Aviv, 69978, Israel
[69]University of Tennessee, Knoxville, Tennessee 37996, USA
[70]University of Texas at Austin, Austin, Texas 78712, USA
[71]University of Texas at Dallas, Richardson, Texas 75083, USA
[72]INFN Sezione di Torino[a]; Dipartimento di Fisica Sperimentale, Università di Torino[b], I-10125 Torino, Italy
[73]INFN Sezione di Trieste[a]; Dipartimento di Fisica, Università di Trieste[b], I-34127 Trieste, Italy
[74]IFIC, Universitat de Valencia-CSIC, E-46071 Valencia, Spain
[75]University of Victoria, Victoria, British Columbia, Canada V8W 3P6
[76]Department of Physics, University of Warwick, Coventry CV4 7AL, United Kingdom
[77]University of Wisconsin, Madison, Wisconsin 53706, USA

We report a search for *CP* violation in the decay $\tau^- \to \pi^- K^0_S\,(\geq 0\pi^0)\,\nu_\tau$ using a dataset of 437 million τ lepton pairs, corresponding to an integrated luminosity of 476 fb^{-1}, collected with the *BABAR* detector at the PEP-II asymmetric energy e^+e^- storage rings. The *CP*-violating decay-rate asymmetry is determined to be $(-0.36 \pm 0.23 \pm 0.11)\%$ approximately 2.8 standard deviations from the Standard Model prediction of $(0.36 \pm 0.01)\%$.

PACS numbers: 13.35.Dx, 11.30.Er

CP violation has been observed only in the K and B meson systems. However, Bigi and Sanda [1] predict that, in the Standard Model (SM), the decay of the τ lepton to final states containing a K^0_S meson will also have a non-zero decay-rate asymmetry due to *CP* violation in the kaon sector. The decay-rate asymmetry

$$A_Q = \frac{\Gamma\left(\tau^+ \to \pi^+ K^0_S\,\overline{\nu}_\tau\right) - \Gamma\left(\tau^- \to \pi^- K^0_S\,\nu_\tau\right)}{\Gamma\left(\tau^+ \to \pi^+ K^0_S\,\overline{\nu}_\tau\right) + \Gamma\left(\tau^- \to \pi^- K^0_S\,\nu_\tau\right)}$$

is predicted to be $(0.33\ \pm 0.01)\,\%$ for decay times comparable to the lifetime $\tau_{K^0_S}$ of the K^0_S meson. In a recent paper, Grossman and Nir [2] point out that Sanda and Bigi did not include the interference between the amplitudes of intermediate K^0_S and K^0_L which is as important as the pure K^0_S amplitude. Therefore the decay-rate asymmetry depends on the reconstruction efficiency as a function of the $K^0_S \to \pi^+\pi^-$ decay time. If the selection is fully efficient for decay times that are long compared with the K^0_S lifetime, then the predicted decay-rate asymmetry is almost unchanged relative to the prediction of Bigi and Sanda [1], due to a sign error [2].

If the measured decay-rate asymmetry shows a significant deviation from the SM value then this could be

*Now at Temple University, Philadelphia, Pennsylvania 19122, USA
†Also with Università di Perugia, Dipartimento di Fisica, Perugia, Italy
‡Now at the University of Huddersfield, Huddersfield HD1 3DH, UK
§Now at University of South Alabama, Mobile, Alabama 36688, USA
¶Also with Università di Sassari, Sassari, Italy

evidence for new physics. No evidence for *CP* violation has been found in related studies by *BABAR* and Belle in $D^+ \to K^0_S\pi^+$ decays [3, 4], by the Belle collaboration in a study of the angular distribution of the decay products in $\tau^- \to \pi^- K^0_S\,\nu_\tau$ decays [5], or by the CLEO collaboration [6].

This paper presents a measurement of A_Q using $\tau^- \to \pi^- K^0_S\,(\geq 0\pi^0)\,\nu_\tau$ and charge conjugate decays. The SM asymmetry is identical for decays with any number of π^0 mesons. If there is an asymmetry due to new-physics dynamics, then the impact of including modes with one or more π^0 mesons may be different.

The analysis uses data recorded by the *BABAR* detector at the PEP-II asymmetric-energy e^+e^- collider, operated at center-of-mass (CM) energies of 10.58 GeV and 10.54 GeV at the SLAC National Accelerator Laboratory. The *BABAR* detector is described in detail in Ref. [7]. In particular, charged kaons and pions are differentiated by ionization (dE/dx) measurements in the silicon vertex detector and the drift chamber in combination with an internally reflecting Cherenkov detector, with identification efficiency greater than 90% for pions and kaons with momenta above 1.5 GeV/c in the laboratory frame [8]. The probability of identifying a pion as a charged kaon is less than 2%. An electromagnetic calorimeter made of cesium iodide crystals provides energy measurements for electrons and photons, and an instrumented flux return detector identifies muons [9]. For momenta above 1 GeV/c in the laboratory frame, electrons and muons are identified with efficiencies of approximately 92% and 70%, respectively. Based on an integrated luminosity of 476 fb^{-1}, the data sample contains approximately 875 million τ leptons.

Simulated event samples are used to estimate the purity of the data sample. The production of τ pairs is simulated with the KK2F Monte Carlo (MC) event generator [10]. Subsequent decays of the τ lepton, continuum $q\overline{q}$ events (where $q = u, d, s, c$), and final-state radiative effects are modeled with Tauola [11], JETSET [12], and PHOTOS [13], respectively. Passage of the particles through the detector is simulated by Geant4 [14].

The τ pair is produced back-to-back in the e^+e^- CM frame. As a result, the decay products of the two τ leptons can be separated from each other by dividing the event into two hemispheres – the "signal" hemisphere and the "tag" hemisphere – using the event thrust axis [15]. The event thrust axis is calculated using all charged particles and all photon candidates in the entire event. We select events with one prompt track and a $K^0_S \to \pi^+\,\pi^-$ candidate reconstructed in the signal hemisphere, and exactly one oppositely charged prompt track in the tag hemisphere. A prompt track is defined to be a track with its point of closest approach to the beam spot being less than 1.5 cm in the plane transverse to the e^- beam axis and less than 2.5 cm in the direction of the e^- beam axis. Furthermore, if a pair of tracks is consistent with coming from a K^0_S or Λ decay, or from a γ conversion after a mass cut and a displaced vertex cut, neither track can be a prompt track. The components of momentum transverse to the e^- beam axis for each of these two prompt tracks must be greater than 0.1 GeV/c in the laboratory frame. The event is rejected if the prompt track in the signal hemisphere is identified to be coming from a charged kaon. A K^0_S candidate is defined as a pair of oppositely charged pion candidates with invariant mass between 0.488 and 0.508 GeV/c^2; furthermore, the distance between the beam spot and the $\pi^+\,\pi^-$ vertex must be at least three times its uncertainty (the $\pi^+\,\pi^-$ will be referred to as the "K^0_S candidate daughters"). To reduce backgrounds from non-τ-pair events, we require that the momentum of the charged particle in the tag hemisphere be less than 4 GeV/c in the CM frame and be identified as an electron (e-tag) or a muon (μ-tag). To reduce backgrounds from Bhabha, $\mu^+\mu^-$, and $q\overline{q}$ events, we require the magnitude of the event thrust to be between 0.92 and 0.99.

Backgrounds from $q\overline{q}$ events are further reduced by rejecting events in which the invariant mass $M_{\rm rec}$ of the charged particle (assumed to be a pion), the K^0_S candidate, and up to three π^0 candidates, all in the signal hemisphere, is greater than 1.8 GeV/c^2 (see Fig. 1). If more than three π^0 candidates are reconstructed in the signal hemisphere, the three with invariant masses closest to the π^0 mass [16] are included in the calculation of $M_{\rm rec}$ and the rest are ignored. The π^0 candidates are constructed from two clusters of energy deposits in the electromagnetic calorimeter that have no associated tracks ("neutral clusters"). The energy of each cluster is required to be greater than 30 MeV in the laboratory frame, and the invariant mass of the two clusters must be between 0.115 GeV/c^2 and 0.150 GeV/c^2. The number of events in the $\tau^- \to \pi^-\,K^0_S\,3\pi^0\nu_\tau$ mode is small and the corresponding invariant mass plot is not included in Fig. 1.

The imperfect agreement between the $M_{\rm rec}$ distributions in the data and MC simulation, seen in Fig. 1, is attributed to strange resonances that are not included in the simulation. The impact of the modeling of the τ decay modes in the MC simulation on the decay-rate asymmetry is found to be small and is included in the systematic uncertainties.

A likelihood ratio $y(\tau)$ is used to distinguish τ-pair events from $q\overline{q}$ events, and a second likelihood ratio $y(K^0_S)$ is used to reduce the background in the sample of $K^0_S \to \pi^+\pi^-$ candidates. The likelihood ratio $y_i\,(\vec{x_i})$, where i refers to τ or K^0_S, is defined as $y_i(\vec{x_i}) \equiv \mathcal{L}^s_i(\vec{x_i})/(\mathcal{L}^s_i(\vec{x_i}) + w\mathcal{L}^b_i(\vec{x_i}))$ where w is the background-to-signal ratio estimated from the MC simulation, $\mathcal{L}^s_i$ ($\mathcal{L}^b_i$) is the likelihood function for signal (background) events, and $\vec{x}_i$ is the set of variables used for likelihood i. Each likelihood function is a product of one-dimensional probability distribution functions of the variables $\vec{x}_i$ obtained from the MC simulation. For $y(\tau)$, the variables $\vec{x}_i$ are the visible energy (sum of the energies associated with all neutral calorimeter clusters and tracks in the event), the number of neutral clusters in the tag hemisphere, the

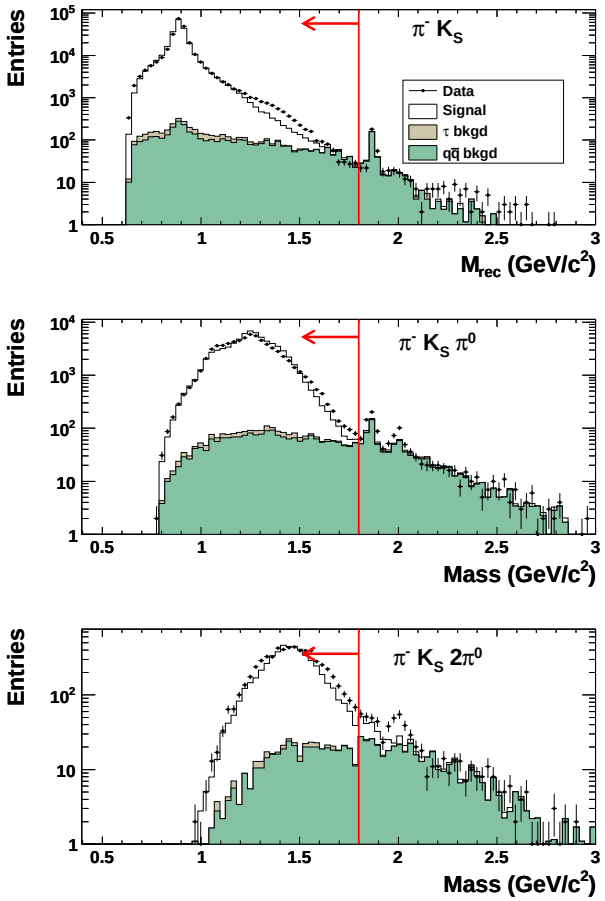

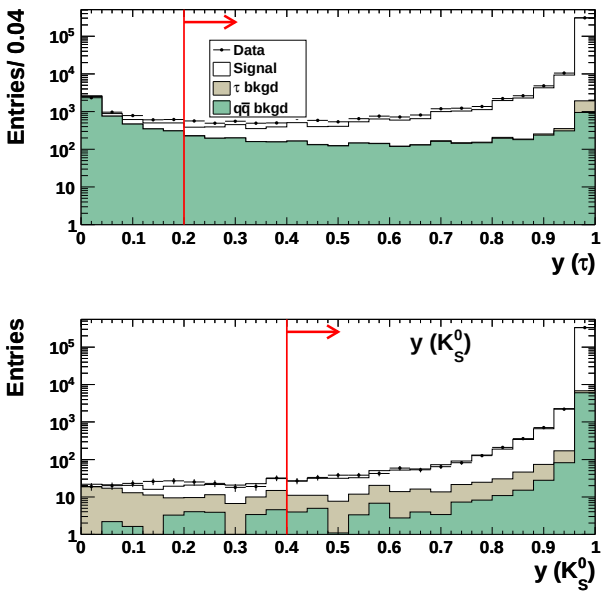

FIG. 2: The likelihood ratio $y(\tau)$ used to distinguish τ events from $q\overline{q}$ events (top plot) and the likelihood ratio $y(K^0_S)$ used to select τ decays with a $K^0_S \to \pi^+\pi^-$ (bottom plot). All selection cuts, except the plotted likelihood ratio requirement, have been applied. Points with error bars represent data while histograms correspond to simulated events. The histogram labeled as "Signal" includes the $\tau^- \to \pi^- K^0_S\,(\geq 0\pi^0)\,\nu_\tau$, residual $\tau^- \to K^- K^0_S(\geq 0\pi^0)\nu_\tau$, and $\tau^- \to \pi^- K^0 \overline{K}^0 \nu_\tau$ modes. The vertical lines indicate the selection criteria.

FIG. 1: Invariant-mass distributions for the combined e-tag and μ-tag samples. The label in each plot indicates the reconstructed decay mode (including the charge conjugate mode). Points with error bars represent data whereas the histograms represent the simulated sample. The histogram labeled as "Signal" includes the $\tau^- \to \pi^- K^0_S\,(\geq 0\pi^0)\,\nu_\tau$, residual $\tau^- \to K^- K^0_S(\geq 0\pi^0)\nu_\tau$, and $\tau^- \to \pi^- K^0 \overline{K}^0 \nu_\tau$ modes. All selection criteria (including the likelihood ratio requirement), except the invariant mass ($M_{\rm rec}$) criterion, have been applied. The vertical lines and arrows indicate the $M_{\rm rec} < 1.8\,{\rm GeV}/c^2$ selection criterion.

number of neutral clusters in the signal hemisphere, the magnitude of the thrust, and the component of the total momentum of the event transverse to the e^- beam axis (calculated from all tracks and neutral clusters in both hemispheres). The variables used to construct $y(K^0_S)$ are the distance from the beam spot to the decay vertex of the K^0_S candidate in the plane transverse to the e^- beam axis, the invariant mass of the K^0_S candidate daughters, the magnitude of the K^0_S momentum, and the cosine of the polar angle of the K^0_S candidate. The polar angle is the angle between the K^0_S trajectory and the e^- beam axis. The cosine of the polar angle discriminates low-angle photon conversions from genuine K^0_S candidates. All kinematic quantities used in the construction of the two likelihood ratios, except for thrust, are determined in the laboratory frame. Events are selected if $y(\tau) > 0.2$ and $y(K^0_S) > 0.4$ (see Fig. 2), in order to minimize the contamination from background events while maintaining a high selection efficiency.

After all selection criteria are applied, a total of 199064 (140602) candidates are obtained in the e-tag (μ-tag) sample, of which there are 99842 (70369) in the τ^- sample and 99222 (70233) in the τ^+ sample.

The sample contains events from two τ decay modes, $\tau^- \to K^- K^0_S(\geq 0\pi^0)\nu_\tau$ and $\tau^- \to \pi^- K^0 \overline{K}^0 \nu_\tau$, that also have K^0_S mesons in the final state. The decay $\tau^- \to \pi^- K^0 \overline{K}^0 \nu_\tau$ satisfies the selection criteria if one of the neutral kaons decays into $\pi^+\pi^-$ and the other neutral kaon decays into $2\pi^0$ or appears as a K^0_L meson.

The selected candidate sample also contains a small background component from τ decays not containing a K^0_S in the final state, as well as continuum $q\overline{q}$ (u, d, s and c-quark) events. There is no background from $B\overline{B}$ events.

The numbers of background events of each type are estimated from the MC simulation. The accuracy of the background estimation is evaluated by measuring the ratios of data to simulated event yields in the region $y(\tau) < 0.1$ and $y(K^0_S) < 0.1$. A correction factor is then applied to the background yield estimated from the Monte Carlo simulation in this region. The correction

factors are determined to be 0.81±0.03 (0.49±0.03) for the $q\overline{q}$ background and 0.9±0.4 (1.0±0.4) for the non-K^0_S τ background in the e-tag (μ-tag) samples, respectively. The total numbers of background events are then estimated to be 1393±79 (1120±65) for τ^- decays and 1401±74 (1055±74) for τ^+ decays in the e-tag (μ-tag) samples, where all selection criteria (including the requirements on the two likelihood ratios) are applied. The uncertainties include the statistical uncertainties from the sizes of the Monte Carlo samples and the uncertainties of the correction factors. The composition of the sample is given Table I.

After the subtraction of background composed of $q\overline{q}$ and non-K^0_S τ decays, the decay-rate asymmetry is measured to be $(-0.32 \pm 0.23)\%$ for the e-tag sample and $(-0.05 \pm 0.27)\%$ for the μ-tag sample, where the errors are statistical.

TABLE I: Breakdown of the sample after all selection criteria have been applied. The errors of the decay modes with K^0_S are dominated by the uncertainties in the branching fractions. The background from other τ decays and $e^+e^- \to q\overline{q}$ background are estimated using the data and MC simulation samples.

Source	Fractions (%)	
	e-tag	μ-tag
$\tau^- \to \pi^- K^0_S(\geq 0\pi^0)\,\nu_\tau$	78.7 ± 4.0	78.4 ± 4.0
$\tau^- \to K^- K^0_S(\geq 0\pi^0)\,\nu_\tau$	4.2 ± 0.3	4.1 ± 0.3
$\tau^- \to \pi^- K^0 \overline{K}^0\,\nu_\tau$	15.7 ± 3.7	15.9 ± 3.7
Other background	1.40 ± 0.06	1.55 ± 0.07

A control sample of $\tau^- \to h^- h^- h^+(\geq 0\pi^0)\,\nu_\tau$ (excluding $K^0_S \to \pi^+\pi^-$ decays) in both data and MC simulation, where h^- (h^+) represents a negatively (positively) charged hadron, is used to confirm that no significant decay-rate asymmetry is induced by the *BABAR* detector or the selection criteria. The control sample is selected by requiring that all charged tracks be prompt tracks, which suppresses K^0_S contamination due to its displaced decay vertex. The asymmetries measured in the simulated and data control samples agree to within the experimental uncertainties of the measurements, which are 0.12% for the e-tag and 0.08% for the μ-tag, and include both statistical and systematic components. These errors are taken as systematic uncertainties on the signal asymmetry (see Table II).

Additional studies show no evidence for any charge-dependent biases in the selection criteria. We find no decay-rate asymmetry in the MC sample of $\tau^- \to \pi^- K^0_S\,(\geq 0\pi^0)\,\nu_\tau$ decays (no *CP* violation is modeled in the simulation) where the error on the decay-rate asymmetries is 0.14% for the e-tag and 0.17% for the μ-tag events. We vary the selection criteria around their nominal values, and no significant changes in the asymmetry are observed. The decay-rate asymmetry of the background events was studied by examining the events rejected by the likelihood ratio criteria and was found to be consistent with zero for both data and MC simulation.

TABLE II: Summary of systematic uncertainties in the decay-rate asymmetries.

	e-tag	μ-tag
Detector and selection bias	0.12%	0.08%
Background subtraction	0.05%	0.06%
$K^0/\overline{K}^0$ interaction	0.01%	0.01%
Total	0.13%	0.10%

A recent paper [17] suggests that the decay-rate asymmetry will be modified due to the different nuclear-interaction cross sections of the K^0 and $\overline{K}^0$ mesons with the material in the detector. This effect is not included in the MC simulation. A correction to the asymmetry accounting for this effect is calculated on an event-by-event basis using the momentum and polar angle of the K^0_S candidate together with the nuclear-interaction cross sections for neutral kaons, which are related by isospin symmetry to the $K^\pm$ nucleon cross sections [16]. The kaon-nucleus cross sections are determined by using the kaon-nucleon cross sections and including a nuclear screening factor of $A^{0.76}$, where A is the atomic weight [17]. The correction, which is subtracted from the measured asymmetry, is found to be $(0.07 \pm 0.01)\%$ for both the e-tag and the μ-tag samples. The error includes the statistical uncertainty in the MC simulation, the uncertainties in the kaon-nucleon cross sections [16], and an uncertainty due to the assumption of isospin invariance. The latter effect is taken to be 5% by observing that isospin symmetry in pion-nucleon cross sections holds to within a few percent. The error on the exponent of the atomic weight of the nuclear screening factor is 0.003 [17] and its contribution to the uncertainty in the asymmetry correction is negligible.

The measured decay-rate asymmetries (after correcting for the difference in neutral kaon nuclear interactions) are $(-0.39 \pm 0.23 \pm 0.13)\%$ for the e-tag sample and $(-0.12 \pm 0.27 \pm 0.10)\%$ for the μ-tag sample, where the first error is statistical and the second is systematic. The systematic uncertainties of the e-tag and μ-tag results are almost completely uncorrelated. The small correlations in the systematic uncertainties for the two samples are ignored when the average is computed. The weighted average of the two decay-rate asymmetries is $(-0.27 \pm 0.18 \pm 0.08)\%$.

The asymmetry measured at this stage still includes other τ decays with K^0_S in the final state. Specifically, the decay-rate asymmetry is diluted due to $\tau^- \to K^- K^0_S\,\nu_\tau$ and $\tau^- \to \pi^- K^0 \overline{K}^0 \nu_\tau$ decays. The measured asymmetry $\mathcal{A}$ is related to the signal asymmetry A_1 and the remain-

ing background asymmetries A_2 and A_3 by:

$$\begin{aligned}\mathcal{A} &= \frac{f_1 A_1 + f_2 A_2 + f_3 A_3}{f_1 + f_2 + f_3} \\ &= \left(\frac{f_1 - f_2}{f_1 + f_2 + f_3}\right) A_Q\end{aligned}$$

where f_1, f_2, and f_3 are, respectively, the fractions of $\tau^- \to \pi^- K^0_S (\geq 0\pi^0)\,\nu_\tau$, $\tau^- \to K^- K^0_S (\geq 0\pi^0)\nu_\tau$, and $\tau^- \to \pi^- K^0 \overline{K}^0 \nu_\tau$ in the total selected sample, shown in Table I. Within the SM, $A_1 = -A_2$ because the K^0_S in $\tau^- \to \pi^- K^0_S\,(\geq 0\pi^0)\,\nu_\tau$ is produced via a $\overline{K}^0$, whereas the K^0_S in $\tau^- \to K^- K^0_S (\geq 0\pi^0)\nu_\tau$ is produced via a K^0. Furthermore, $A_3 = 0$ in the SM because the asymmetries due to the K^0 and $\overline{K}^0$ will cancel each other. Using the relations between A_1, A_2, and A_3, we can compare our result with the theoretical prediction by dividing the measured decay-rate asymmetry of $\mathcal{A} = (-0.27 \pm 0.18 \pm 0.08)\%$ by $(f_1 - f_2)/(f_1 + f_2 + f_3) = 0.75 \pm 0.04$ (the correction is identical for the e-tag and μ-tag samples). The uncertainty on the correction includes the statistical uncertainty and uncertainties in the branching fractions. Finally, the decay-rate asymmetry for the $\tau^- \to \pi^- K^0_S\,(\geq 0\pi^0)\,\nu_\tau$ decay for the combined e-tag and μ-tag sample is calculated to be $A_Q = (-0.36 \pm 0.23 \pm 0.11)\%$.

As pointed out by Grossman and Nir, the predicted decay-rate asymmetry is affected by the $K^0_S \to \pi^+\pi^-$ decay time dependence of the event selection efficiency [2]. Figure 3 shows the relative selection efficiency, defined as the selection efficiency normalized to unity in the range $0.25 < t/\tau_{K^0_S} < 1.0$. In the $0 < t/\tau_{K^0_S} < 1$ region, the relative efficiency is parametrized with the function $\left(1 - Ae^{-B(t-t_0)}\right)^{-2}$, where A, B, and t_0 are constants. In the $1 < t/\tau_{K^0_S} < 8$ region, the relative efficiency is parametrized by a second-order polynomial. Both functions are constrained to unity at $t/\tau_{K^0_S} = 1$. We use this parametrization in Eq. (13) of the Grossman and Nir paper [2] to obtain a multiplicative correction factor of 1.08 ± 0.01 for the decay-rate asymmetry, where the error is due to the uncertainty in the relative selection efficiency. After applying the correction factor, the SM decay-rate asymmetry is predicted to be $(0.36 \pm 0.01)\%$.

In conclusion, we have performed a search for *CP* violation using the $\tau^- \to \pi^- K^0_S\,(\geq 0\pi^0)\,\nu_\tau$ decay mode. The decay-rate asymmetry is measured for the first time and is found to be $(-0.36 \pm 0.23 \pm 0.11)\%$. The measurement is 2.8 standard deviations from the SM prediction of $(0.36 \pm 0.01)\%$.

The authors thank Y. Grossman and Y. Nir for their useful suggestions. We are grateful for the excellent luminosity and machine conditions provided by our PEP-II colleagues, and for the substantial dedicated effort from the computing organizations that support *BABAR*. The collaborating institutions wish to thank SLAC for its support and kind hospitality. This work is supported by DOE and NSF (USA), NSERC (Canada), CEA and CNRS-IN2P3 (France), BMBF and DFG (Germany), INFN (Italy), FOM (The Netherlands), NFR (Norway), MES (Russia), MICIIN (Spain), STFC (United Kingdom). Individuals have received support from the Marie Curie EIF (European Union), the A. P. Sloan Foundation (USA) and the Binational Science Foundation (USA-Israel).

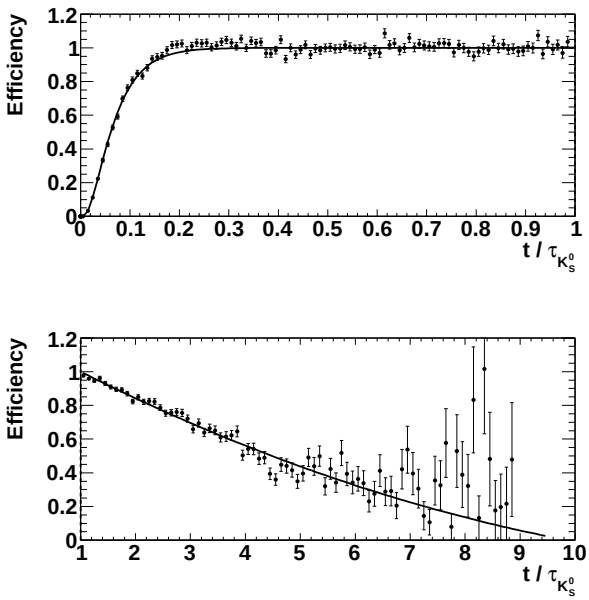

FIG. 3: The relative selection efficiency as a function of $t/\tau_{K^0_S}$ obtained from the Monte Carlo sample. The top plot shows the region $0 < t/\tau_{K^0_S} < 1$ and the bottom plot the region $1 < t/\tau_{K^0_S} < 8$. The solid line is the fit to the points in the displayed region. The relative efficiency is normalized to be unity for the region $0.25 < t/\tau_{K^0_S} < 1.0$.

[1] I. I. Bigi and A. I. Sanda, Phys. Lett. B **625**, 47 (2005).
[2] Y. Grossman and Y. Nir, arXiv:1110.3790 [hep-ph] (2011).
[3] P. del Amo Sanchez *et al.* (*BABAR* Collaboration), Phys. Rev. D **83**, 071103 (2011).
[4] B. R. Ko *et al.* (Belle Collaboration), Phys. Rev. Lett. **104**, 181602 (2010).
[5] M. Bischofberger *et al.* (Belle Collaboration), Phys. Rev. Lett. **107**, 131801 (2011).
[6] G. Bonvicini *et al.* (CLEO Collaboration), Phys. Rev. Lett. **88**, 111803 (2002).
[7] B. Aubert *et al.* (*BABAR* Collaboration), Nucl. Instr. Methods Phys. Res., Sect. A **479**, 1 (2002).
[8] B. Aubert *et al.* (*BABAR* Collaboration), Phys. Rev. Lett. **99**, 021603 (2007).
[9] J. P. Lees *et al.* (*BABAR* Collaboration), Phys. Rev. D **81**,

111101(R) (2010).
[10] B. F. L. Ward, S. Jadach, and Z. Was, Nucl. Phys. Proc. Suppl. **116**, 73 (2003).
[11] S. Jadach *et al.*, Comput. Phys. Commun. **76**, 361 (1993).
[12] T. Sjostrand, Comput. Phys. Commun. **82**, 74 (1994).
[13] E. Barberio and Z. Was, Comput. Phys. Commun. **79**, 291 (1994).
[14] S. Agostinelli *et al.*,(Geant4 Collaboration) Nucl. Instr. Methods Phys. Res., Sect. A **506**, 250 (2003).
[15] S. Brandt *et al.*, Phys. Lett. **12**, 57 (1964); E. Farhi, Phys. Rev. Lett. **39**, 1587 (1977).
[16] K. Nakamura *et al.* (Particle Data Group), J. Phys. **G 37**, 075021 (2010) and 2011 partial update for the 2012 edition.
[17] B. R. Ko *et al.*, arXiv:1006.1938 [hep-ex] (2010).